

Functionalizing Luminescent Metal–Organic Frameworks for Enhanced Photoluminescence

Xiao-Yuan Liu,[†] William P. Lustig,[†] and Jing Li*



Cite This: *ACS Energy Lett.* 2020, 5, 2671–2680



Read Online

ACCESS |

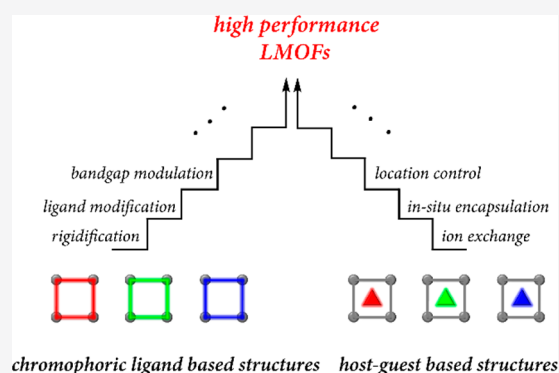


Metrics & More



Article Recommendations

ABSTRACT: Luminescent metal–organic frameworks (LMOFs) have received considerable attention in recent years because of their enormous potential for a broad range of applications in chemical sensing, energy-efficient lighting, bioimaging, and related fields. Benefiting from their tunable crystal structures, compositions, and porosity, significant progress has been made in developing LMOFs with high luminescence quantum efficiency. In this Perspective, we highlight two recently developed strategies that have been successful in designing LMOFs that are made of chromophoric ligands or that encapsulate emissive guest species. These LMOFs offer the highest photoluminescence performance and most flexibility in tuning emission energy and colors. We also discuss the main challenges as well as new opportunities for the future development of LMOFs.



Luminescent metal–organic frameworks (LMOFs) are well-known for research into their applications in chemical sensing,^{1–7} lighting,^{8–13} bioimaging,^{14,15} and various related fields.^{16–18} Investigation of these functional materials seeks to take advantage of their tunable structures and compositions, permanent porosity, and diverse chemical and physical properties. LMOFs can be roughly divided into three categories based on the source of their luminescence: metal nodes/clusters,^{19–23} chromophoric ligands,^{9,24–29} and guest species.^{8,10,12,13,30} Accordingly, a number of comprehensive reviews have been published which discuss the synthesis, crystal structures, optical properties, emission mechanisms, and applications of LMOFs.^{1,21,31–38} One emerging area of research is the development of these materials as alternative phosphors for energy-efficient lighting technologies that are free of rare-earth elements (REEs), more eco-friendly, and earth abundant. While this subfield has been progressing very rapidly, and many LMOFs have been synthesized in the past several years, significant challenges and limitations remain to be addressed. These include lack of long-term photostability and insufficient photoluminescence quantum yield (PLQY). A majority of the compounds can be excited only by high-energy UV light sources, making them incompatible with the current white-light-emitting diodes (WLEDs) that use blue light chips (e.g., 450 nm). Clearly, new strategies and/or methods are required to overcome these shortcomings in order to meet the standard for commercialization. Among a variety of possibilities, the two very recently developed approaches involve the construction of LMOFs from highly emissive chromophoric

ligands and encapsulation of luminescent guest species into the MOF pores. These LMOFs offer the highest luminescence quantum efficiency and emission color tunability. In this Perspective, we will highlight the current progress of these approaches, with a focus on the most recent work of our own. We will briefly discuss the existing challenges and future perspectives for designing and synthesizing LMOFs that are specifically promising as alternative LED phosphors.

Chromophoric Ligand-Based LMOFs. The chromophoric ligand-based LMOFs can have extremely high quantum yields for single-color emission, with the best reported performances reaching internal quantum yields (IQYs) of nearly 100%.^{25–27,39} This high luminescence efficiency is due to a number of factors, with rigidification of the chromophore ligands playing a major role.^{9,24,25} These chromophoric ligands are typically designed based on high-performance organic chromophores, and when they are linked to form the rigid framework of the material, vibrational and rotational modes that lead to nonradiative relaxation pathways to the chromophore can be removed or diminished, thereby enhancing photoemissions. However, it should be noted that

Received: May 25, 2020

Accepted: July 20, 2020

Published: July 20, 2020



this is not always the case; if the framework is such that ligand movement is allowed, the lack of rigidity can cause a severe drop in luminescence efficiency.

The chromophoric ligand-based LMOFs can have extremely high quantum yields for single-color emission, with the best reported performances reaching internal quantum yields of nearly 100%. This high luminescence efficiency is due to a number of factors, with rigidification of the chromophore ligands playing a major role.

The impact of framework rigidification on luminescence efficiency in chromophoric-ligand-based LMOFs was recently explored using a model composed of two isorecticular LMOFs, LMOF-263 [$\text{Zn}_2(\text{tcbe})(\text{bpy})$, H_4tcbe = 1,1,2,2-tetrakis(4-(4-carboxy-phenyl)phenyl)ethene, bpy = 4,4'-bipyridine] and LMOF-301 [$\text{Zn}_2(\text{tcbe-F})(\text{bpy})$, $\text{H}_4\text{tcbe-F}$ = 1,1,2,2-tetrakis(4-(4-carboxy-3-fluoro-phenyl)phenyl)ethene].⁴⁰ The two LMOFs are constructed from nearly identical ligands and have precisely the same connectivity; the only difference between them is the replacement of four hydrogen atoms on the chromophoric tcbe ligand with fluorine (Figure 1a). In both cases, the chromophoric ligands (tcbe in LMOF-263 and tcbe-F in LMOF-301) form a two-dimensional (2D) layered structure with the Zn^{2+} paddlewheel secondary building units (SBUs). These layers are further linked by pillaring bpy ligands to generate a three-dimensional (3D) framework, and two of these frameworks interpenetrate to yield the complete MOF structure (Figure 1b–d).

When these MOFs are outgassed, the fluorine atoms on the tcbe-F ligand in LMOF-301 prevent rotation of a bipyridyl phenyl group, while in the nonfluorinated LMOF-263, the bipyridyl group becomes free to spin. This increased rotational freedom causes the quantum yield of LMOF-263 to plummet from 42.5% in the as-made sample to 12.2% in the outgassed sample. On the other hand, the quantum yield of the more rigid LMOF-301 only drops from 50.9% to 45.1% upon outgassing.⁴⁰ This significant difference in luminescent efficiency being directly linked to framework flexibility provided an opportunity to study postsynthetic strategies for boosting quantum yield by increasing framework rigidity. This is attractive because finding a reliable way to postsynthetically rigidify ligands in an LMOF may be generalizable and cost-effective, potentially providing a tool that could be widely used to improve luminescent performance.

A solvent-loading approach was used, in which the outgassed LMOF samples were soaked in a variety of solvents with varying molecular shape, size, and chemical properties, and it was found that the greatest improvement in quantum yield was achieved by immersing the LMOF samples in *n*-pentane; the quantum yield of outgassed LMOF-263 increased from 12.2% to 59.3%, while the quantum yield of outgassed LMOF-301 increased from 45.1% to 48.5%.⁴⁰ PXRD analysis was made for all samples, and it was found that the unit cell of the LMOFs changed upon absorbing *n*-pentane, expanding in the *c* direction while contracting in the *b* direction. This is consistent with a shifting in the positions of the two interpenetrated nets

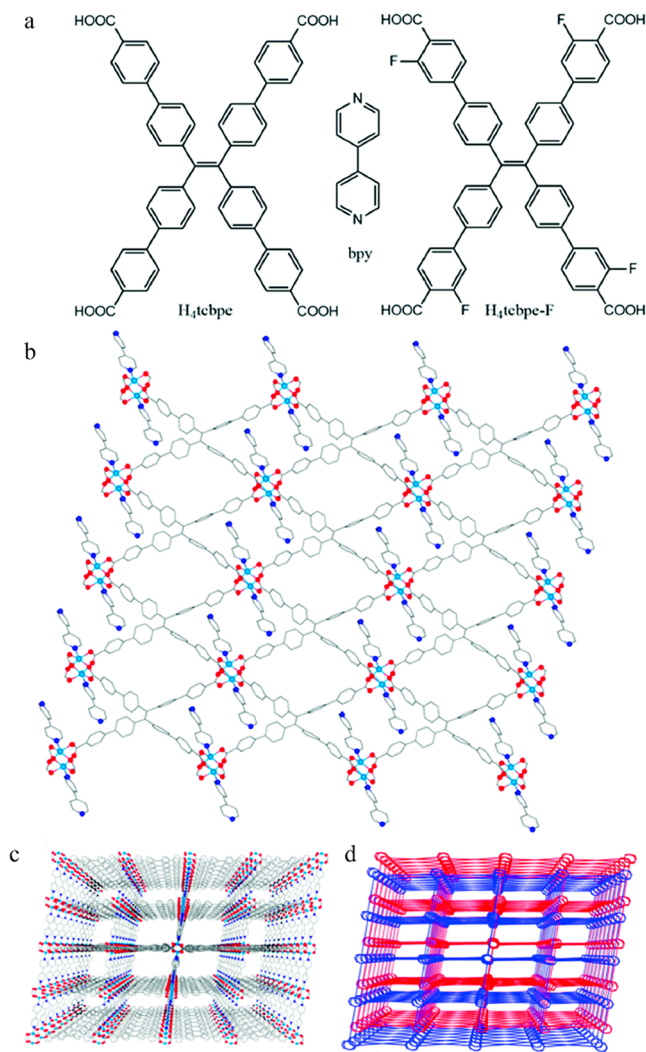


Figure 1. (a) Structures of the ligands H_4tcbe , bpy , and $\text{H}_4\text{tcbe-F}$. (b) 2D sheet of tcbe ligands in the bc plane linked by zinc paddlewheel SBUs, showing pillaring bpy ligands extending above and below the sheet. (c) Single 3D net of LMOF-263. (d) Schematic of two interpenetrated nets (red and blue), giving the final structure of LMOF-263. C, gray; O, red; N, dark blue; Zn, light blue. Hydrogen atoms have been omitted for clarity. Copyright 2019, Royal Society of Chemistry. Reproduced with permission from ref 40.

that would prevent rotation of the bipyridyl phenyl ring in LMOF-263 (Figure 2). This work not only emphasizes the importance that framework rigidity plays on LMOF luminescence but also demonstrates that substantial quantum yield gains can be realized through guest-mediated rigidification. Because porosity is so common in MOFs, this technique has the potential to boost quantum yield in a significant proportion of LMOFs.

The importance of understanding luminescence mechanisms in designing high-performance LMOFs with a chromophoric-ligand strategy is also emphasized by another recent work.⁴¹ Being a chromophore-based MOF, outgassed LMOF-231 [$\text{Zn}_2(\text{tcbe})$] had held the record for the highest quantum yield among yellow-emitting LMOFs under blue excitation since 2015, with an emission peak centered at 550 nm and an IQY of 76% under 455 nm (blue) excitation;²⁵ however, it has an even higher IQY of 95% under the excitation at 420 nm

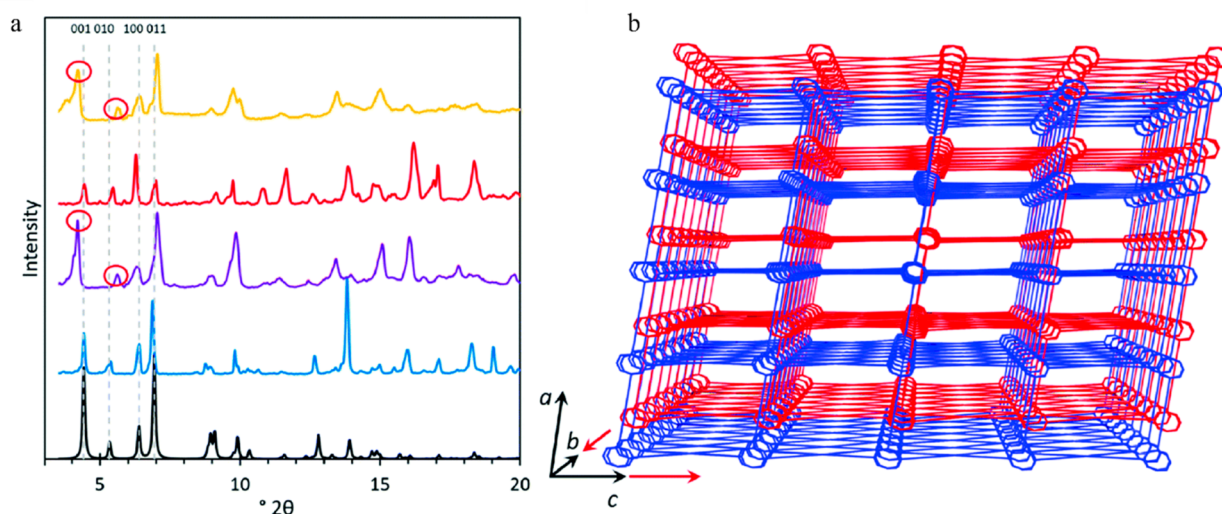


Figure 2. (a) Simulated PXRD pattern of LMOF-263 (black) overlaid with the PXRDs of the activated LMOF-263 (blue), activated LMOF-301 (red), pentane-loaded LMOF-263 (purple), and pentane-loaded LMOF-301 (gold). The first four peaks are indexed, and the peak changes observed in the pentane-loaded samples are marked with red circles. As LMOF-263 and LMOF-301 are isorecticular with nearly identical unit cells, only the simulated pattern for LMOF-263 is shown. (b) A crystallographic shift that could be responsible for the expansion along the *c*-axis and contraction along the *b*-axis observed in the pentane-loaded samples. Copyright 2019, Royal Society of Chemistry. Reproduced with permission from ref 40.

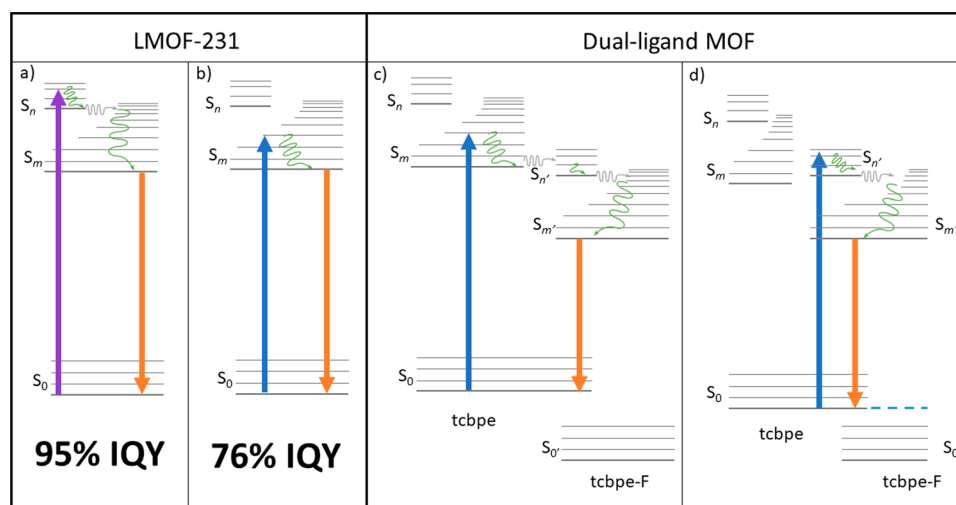


Figure 3. (a) Schematic illustrating a possible fluorescence mechanism for the more efficient "higher-energy pathway" in LMOF-231 following absorbance of a 420 nm photon. (b) Schematic illustrating a possible fluorescence mechanism for the less efficient "lower-energy pathway" in LMOF-231 following absorbance of a 455 nm photon. (c) Schematic demonstrating a possible fluorescence mechanism in a dual-ligand MOF composed of both tcbpe and tcbpe-F, in which absorbance of a 455 nm photon on tcbpe is followed by electron transfer to a neighboring tcbpe-F. (d) Another possible mechanism, in which absorbance of a 455 nm photon results in direct excitation from tcbpe to tcbpe-F, injecting an excited electron directly in to the "higher-energy pathway". Copyright 2020, Royal Society of Chemistry. Reproduced with permission from ref 41.

(violet). A spectroscopic investigation of the luminescence mechanism was made to investigate why higher-energy excitation was more efficient and determine if there was a way to boost the IQY under blue excitation to a similar level. Photoluminescence lifetime data collected from outgassed LMOF-231 under 380 and 440 nm excitation indicated that two competing pathways for exciton recombination existed: a faster process and a slower process. Under 380 nm excitation, the faster process dominated, while under 440 nm excitation, the slower process dominated. To improve the quantum efficiency under blue excitation in LMOF-231, it was therefore

necessary to shift more exciton recombination to the faster process.

Because of the large Stokes shift exhibited by LMOF-231 and the fact that the emission energy of the LMOF is independent of excitation energy, it was likely that electrons are being excited from the LMOF's highest occupied molecular orbital (HOMO) to some energy level that was significantly higher than the lowest unoccupied molecular orbital (LUMO). The electrons then relax down to the LUMO, where they emit. The primary difference between violet and blue excitation is that the former has a larger Stokes shift and must therefore excite the electron into a higher initial energy level than blue

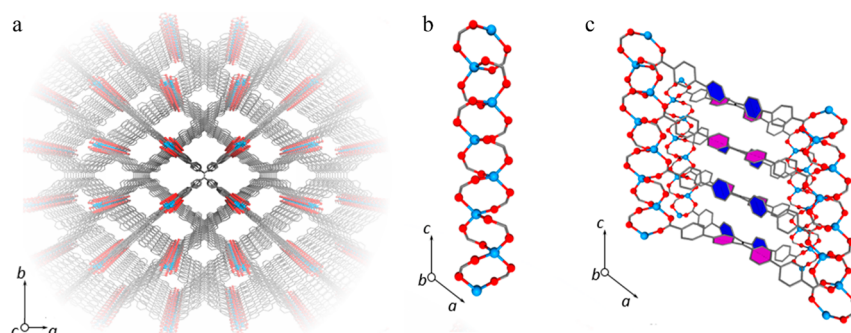


Figure 4. (a) The complete structure of LMOF-231 viewed along the *c* axis. (b) A segment of LMOF-231's infinite secondary building unit, which runs parallel to the *c* axis. (c) A section of LMOF-231 viewed along the *b* axis, showing a single column of tcbpe ligands linking four zinc-carboxylate chains parallel to the *c* axis. Pink-colored phenyl rings indicate an ethene-phenyl dihedral angle of 42.2°, while blue-colored phenyl rings indicate an ethene-phenyl dihedral angle of 58.7°. Copyright 2020, Royal Society of Chemistry. Reproduced with permission from ref 41.

excitation (Figure 3a,b). In order to reach this same higher initial energy level under blue excitation, and thereby shift the emission pathway toward the faster process described above, a bandgap modulation strategy was used. DFT calculations showed that fluorinated tcbpe (tcbpe-F) has an effectively identical bandgap to nonfluorinated tcbpe, with the HOMO and LUMO energy levels in tcbpe-F offset by -0.22 eV and -0.23 eV, respectively, relative to tcbpe. This offset, coupled with the similar electronic structure of the two nearly identical ligands, could decrease the energy level required to reach that higher-lying energy state (Figure 3c,d). Emission from such a bandgap-modulated structure would likely result from a combination of intramolecular (Figure 3b) and intermolecular (Figure 3c,d) processes.⁴¹

This bandgap modulation strategy was established for LMOF-231; zinc carboxylate chains run along the *c*-axis of the crystal structure, with the chromophoric tcbpe ligands that link four of these chains together organized into closely packed stacks (Figure 4). The short distance (5.4 Å) between ligands in the stack permit electronic interaction, while the twisted ring conformation prevents π - π stacking that could otherwise cause emission quenching.⁴¹

Following the strategy described above, tcbpe-F was doped into LMOF-231 at 20% loading to create LMOF-305 (Zn_2 tcbpe_{0.8} tcbpe-F_{0.2}). As desired, the internal quantum yield of LMOF-305 under 455 nm excitation was increased to 88%, a nearly 12% enhancement relative to that of LMOF-231 (76%). To determine if this increase in quantum yield was accomplished via the intended change in emission discussed above, photoluminescent lifetime data was collected under 380 and 440 nm excitation to establish if emission from outgassed LMOF-305 under blue excitation was pushed toward the faster pathway, and polarized photoluminescence measurements were collected to understand how neighboring ligands interacted during luminescence, which was relevant because the bandgap modulation strategy was based upon the theory that luminescence processes would involve neighboring tcbpe and tcbpe-F ligands.

Lifetime data show that emission from outgassed LMOF-305 under 440 nm excitation favors the faster process by a factor of 2:1, while outgassed LMOF-231 favors the slower process by a factor of 2:1 under the same conditions. Unlike LMOF-231, the average amplitude weighted lifetime, the lifetimes of both the fast and the slow process, and the relative weighting of the two processes in LMOF-305 are closely

matched under both violet and blue excitation. This demonstrates that bandgap modulation strategy successfully altered the emission mechanism of LMOF-305 under blue excitation to more closely match the high-efficiency emission mechanism of the LMOF under violet excitation. Outgassed LMOF-305 has the highest quantum yield of any blue-excitable yellow-emitting LMOF phosphor. Its development relied on identifying and understanding luminescence processes and demonstrates the strong potential that in-depth spectroscopy and computational approaches have in rationally designing LMOF phosphors.

Host-Guest-Based LMOFs. One of the defining characteristics of metal-organic frameworks is their porosity. Guest-containing LMOFs take advantage of this to load luminescent guest species into their pores. Additionally, the fact that the guest molecules contribute to luminescence can enable more design flexibility in developing the LMOFs, because it may not be necessary to achieve the maximum possible luminescent efficiency from the framework; framework design can instead prioritize other important properties such as stability and morphology. Because these LMOFs can have multiple emission centers, they are well-suited to developing lighting phosphors with broad spectral coverage, and because the emission color can depend upon the relative abundance of the various emission centers, emission can be easily balanced by modulating the amount of luminescent guest(s) present in the reaction mixture. Finally, unlike chromophore-based LMOFs, it is generally not necessary to adapt known phosphor structures to permit their inclusion into the MOF, because they are guest molecules and not part of the framework.

For the host-guest-based LMOFs, the most commonly adopted preparation method is through postsynthesis modification. The pristine MOFs are first synthesized, and the guests are loaded into the pores via diffusion or ion exchange.^{30,42} Because of the separate processes of the MOF synthesis and guests encapsulation, a wide variety of MOFs can be used as the hosts. Experimental conditions are then developed which offer good guest solubility while having no effect on the MOF structures; these conditions are used to place guests inside the pores. A major advantage of this strategy is that the confinement and isolation of photoluminescent guests into the pores can significantly reduce aggregation-caused fluorescence quenching, enhancing the guest's photoluminescent properties. Accordingly, various guest@MOFs have been synthesized with excellent PLQYs,

One of the defining characteristics of metal–organic frameworks is their porosity. Guest-containing LMOFs take advantage of this to load luminescent guest species into their pores. Additionally, the fact that the guest molecules contribute to luminescence can enable more design flexibility in developing the LMOFs, because it may not be necessary to achieve the maximum possible luminescent efficiency from the framework; framework design can instead prioritize other important properties such as stability and morphology.

as summarized in Table 1. However, some serious limitations exist for this strategy. First, because the guest molecules enter the pores after the pristine MOF formation, they can also easily leak out of the same pore aperture. In order to permanently trap the guests inside pristine MOFs, the molecular dimensions of the guests must be small enough to fit in the cavity yet larger than the pore aperture/opening. Second, the crystal sizes of MOFs are often larger than a micrometer, which poses device fabrication challenges for lighting applications. The *in situ* encapsulation of guest species into nanosized core/shell MOFs to form nanocomposites is a promising alternative approach that can overcome these limitations and provide a new platform for the design and synthesis of LMOFs with optimal luminescent properties and high efficiency.

The *in situ* encapsulation of guest species into nanosized core/shell MOFs to form nanocomposites is a promising alternative approach that can overcome these limitations and provide a new platform for the design and synthesis of LMOFs with optimal luminescent properties and high efficiency.

In a very recent work, we demonstrated how this approach works. Three host–guest-based dye@MOF models, namely, multiphase single-shell, single-phase single-shell, and single-phase multishell, were built to tune and enhance the emission behavior of resulting MOF nanocomposites. In these models, various guests that emit different colors were added into the MOF precursor solutions separately, together, or one-by-one (Figure 5a).⁴⁹ By doing so, guest location control could be exercised by encapsulating them into different MOF shells to generate the desired emission colors, while reducing guest-interaction-induced fluorescence quenching. In the initial study, ZIF-8 was selected as the host according to the following reasons: (i) ZIF-8 can be synthesized in water, methanol, and DMF under mild conditions, which allows a

broader choice of guest species; (ii) the synthesis of nanosized ZIF-8 crystals with controlled morphology has been reported;⁵¹ (iii) the encapsulation of multiple components into multishelled ZIF-8 with controlled guest location has been established.⁵² More importantly, to effectively encapsulate guests into the cavity of ZIF-8 during synthesis and avoid their leakage after synthesis, we chose rhodamine B (RB), fluorescein (F), and 7-amino-4-(trifluoromethyl)-coumarin (C-151) as the guests (Figure 5c–e) to ensure the dimensions of these dye molecules are larger than the window size of ZIF-8 but smaller than the cavity size. The molecular sizes of C-151, F, and RB are $\sim 8.0 \times 11.0$, 11.0×13.0 , and 10.2×16.8 Å, respectively. The aperture of the pore window and the cage size of ZIF-8 are ~ 3.40 Å and ~ 11.6 Å (Figure 5b); all three guests can therefore be effectively trapped inside the ZIF-8 cages.

In model one, uniform RB@ZIF-8, F@ZIF-8, and C-151@ZIF-8 nanocomposites with crystal diameters less than 200 nm and orange, green, and blue emission were prepared by directly adding the dye molecules into the synthesis solution of ZIF-8 (Figure 5f–h). When compared with the free dye fluorophores, a significant enhancement in quantum yield was observed, as a result of reduced aggregation-caused quenching achieved by confining and isolating the dye molecules within individual ZIF-8 pores. This result demonstrated that the *in situ* encapsulation method is an effective way to prepare nanosized MOF-based materials via *in situ* synthesis. By mixing the three kinds of nanocomposites together at the appropriate ratio, white-light emission can also be realized with a CIE coordinate (0.32, 0.34).

By adding the three guests simultaneously into the ZIF-8 precursors (model two), nanosized RB&F&C-151@ZIF-8 was prepared, and white-light emission can also be achieved after adjusting the encapsulated ratios of three dyes. However, it should be noted that for the single-phase single-shell RB&F&C-151@ZIF-8 nanocomposites, strong fluorescent resonance energy transfer may significantly decrease the quantum efficiency of the dye molecules, as well as the nanocomposite material considered as a whole. Therefore, to reduce fluorescence resonance energy transfer between the selected guests and maximize the luminescence efficiency, the single-phase multishell composite (model three) was synthesized, where the three dyes were added into the ZIF-8 precursors solution one-by-one during the shell-by-shell overgrowth. This procedure effectively separates the dye molecules from each other spatially. By sequential encapsulation of the three dyes, the emission can be tuned from blue through white to orange under UV excitation. This work clearly demonstrates that the *in situ* encapsulation is a useful approach to form solution-processable nanocomposites with tunable emission behavior and enhanced luminescence efficiency.

To confirm the universality of the *in situ* encapsulation strategy and to realize white-light emission via a blue light excitable yellow phosphor, UiO-66 was then selected as the host and 4,9-dibromonaphtho[2,3-c][1,2,5]thiadiazole (DBNT) as the yellow emitting guest (Figure 6a,b).⁵⁰ The resulting nanosized DBNT@UiO-66 shows enhanced photoluminescent intensity under blue light excitation (Figure 6c,d). Bright white-light emission can be achieved by coating this nanocomposite onto a blue light LED chip. This work confirms that the *in situ* encapsulation strategy can be employed to other types of MOFs, and that blue-light excitable

Table 1. Summary of Host–Guest-Based LMOFs

MOF	guest molecule	synthesis method	crystal size	color	IQY% (λ_{ex})
$[(CH_3)_2NH_2]_{15}[(Cd_2Cl)_3(TATPT)_4] \cdot 12DMF \cdot 18H_2O$ ^a	$[Ir(ppy)_2(bpy)]PF_6$	ion exchange	micro	white	20.4 (370 nm)
ZIF-8 ⁴³	CDs	<i>in situ</i>	nano	green	
ZIF-90 ¹⁴	RB ^b	<i>in situ</i>	nano		
NENU-521 ⁴⁴	Alq3 ^c	diffusion	micro	white	11.4 (370 nm)
Al-DBA ^{45,d}	RB	diffusion	nano	white	12 (365 nm)
HSB-W1 ³⁰	DCM ^e	diffusion	micro	red	27.1 (365 nm)
	C6 ^f			green	21 (365 nm)
	CBS-127 ^g			blue	54.4 (365 nm)
	DCM&C6&CBS-127			white	26 (365 nm)
bio-MOF-1 ⁴⁶	RB	ion exchange	micro	red	68 (450 nm)
	R110			yellow-green	79 (450 nm)
	R6G			orange	49 (450 nm)
	R123			yellow	66 (450 nm)
ZJU-28 ^{10,42}	DSM ^h	ion exchange	micro	orange	60.7 (365 nm)
	AF ⁱ			green	
	DSM&AF			white	17.4 (365 nm)
	C6&R6G&R101	diffusion		white	82.9 (460 nm)
CD-MOF ¹²	7-HCm ^j	diffusion	micro	blue	
	F ^k			green	95 (478 nm)
	RB			yellow	82 (470 nm)
	7-HCm&F&RB			white	
LIFM-WZ-6 ¹³	RB	diffusion	micro	red	10.9 (365 nm)
	BR-2 ^l			blue	6.8 (365 nm)
	APFG ^{++m}			pink	7.8 (365 nm)
NENU-524 ⁴⁷	$[Ir(ppy)_2(bpy)]^+$	ion exchange	micro	white	15.2 (365 nm)
ZIF-8 ⁴⁸	PM605	ion- and liquid-assisted grinding/accelerated aging		yellow	67.5 (467 nm)
	PM546			green	
	HClBOH			orange	
	PM650			pink	
ZIF-8 ⁴⁹	C-151 ⁿ	<i>in situ</i>	nano	blue	41.9 (365 nm)
	F			green	62.6 (365 nm)
	RB			orange	60.1 (365 nm)
ZIF-8 ⁵⁰	R6G	<i>in situ</i>	nano	yellow	63.1 (450 nm)
UiO-66 ⁵⁰	DBNT ^o	<i>in situ</i>	nano	yellow	22.7 (450 nm)

^aH₆TATPT: 2,4,6-tris(2,5-dicarboxylphenyl-amino)-1,3,5-triazine. ^bRB: rhodamine B. ^cAlq3:tris(8-hydroxy quinoline)aluminum. ^dDBA: 9,10-dibenzoate anthracene. ^eDCM: 4-(dicyanomethylene)-2-methyl-6-(p-dimethylaminostyryl)-4H-pyran. ^fC6: Coumarin 6. ^gCBS-127: fluorescent brightener. ^hDSM: 4-(p-dimethylaminostyryl)-1-methylpyridinium. ⁱAF: acriflavine. ^j7-HCm: 7-hydroxycoumarin. ^kF: fluorescein. ^lBR-2⁺: basic red 2. ^mAPFG⁺: Astrazon pink FG. ⁿC-151: 7-amino-4-(trifluoromethyl)-coumarin. ^oDBNT: 4,9-dibromonaphtho[2,3-c][1,2,5]thiadiazole.

yellow dye@MOF nanocomposites can generate high-quality white light.

Combining the facile and scalable synthesis of nanosized MOFs and the use of low-cost, commercially available guest species, the *in situ* encapsulation of strongly emissive molecules offers a novel and efficient approach for making solution-processable, high-performance, and systematically tunable light-emitting nanocomposite materials that are promising

candidates for use as a new family of phosphors in energy-efficient lighting devices.

Summary and Future Outlook. In this Perspective, we briefly summarize the two recently developed strategies to synthesize low-cost and high-performance LMOFs based on chromophoric ligands and *in situ* guest encapsulation. Although many LMOFs have been reported, the tunable structures and properties of this material class provide ample opportunities

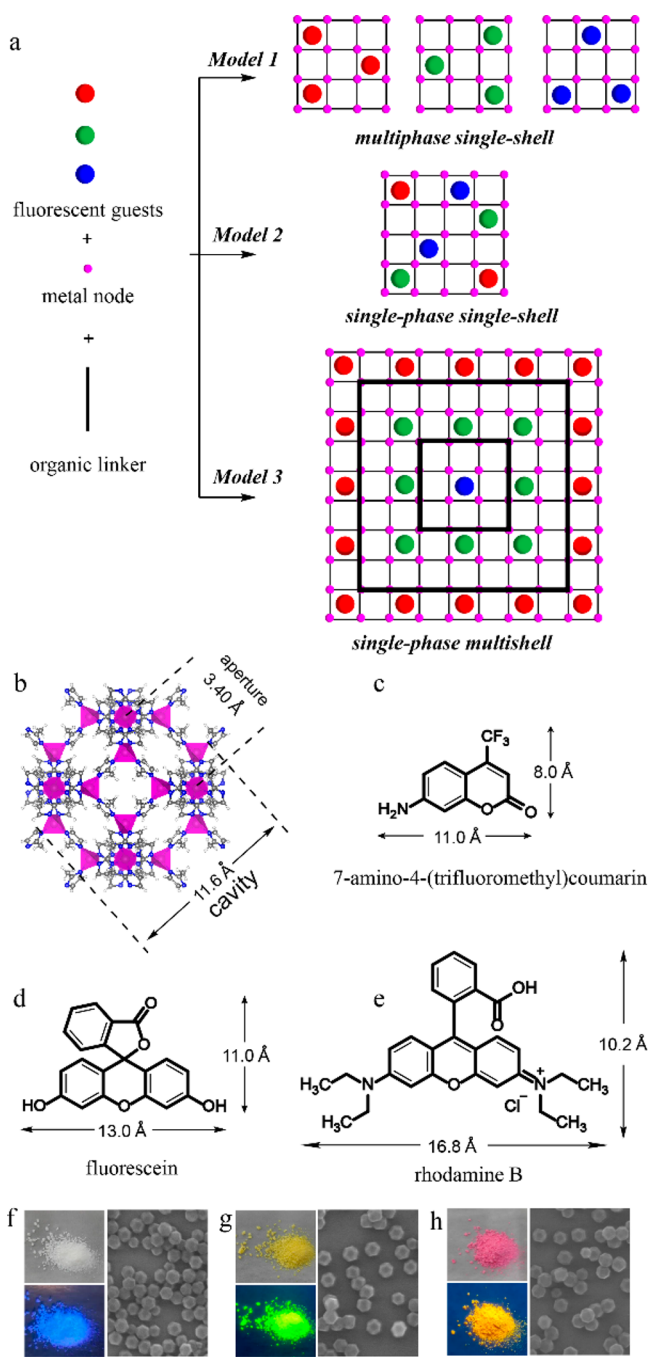


Figure 5. (a) Schematic showing three models for the preparation of fluorescent guest encapsulated MOF nanocomposites. (b) Crystal structure of ZIF-8. The aperture and cage sizes are indicated in the plot. (c–e) Molecular structures and dimensions of 7-amino-4-(trifluoromethyl)coumarin (C-151), fluorescein (F), and rhodamine B (RB). (f–h) The images of C-151@ZIF-8², F@ZIF-8², and RB@ZIF-8² nanocomposites under daylight (top left), photoexcitation (bottom left), along with their corresponding SEM images (right, scale bar: 200 nm).

for additional improvement in their synthesis and application development as well as in tackling unmet challenges and obstructions which must be addressed in order to maximize their potential for practical applications. In this regard, we propose several promising areas of research which can further accelerate the development of chromophoric ligand-based, host–guest-based, and nanosized LMOFs. We believe that

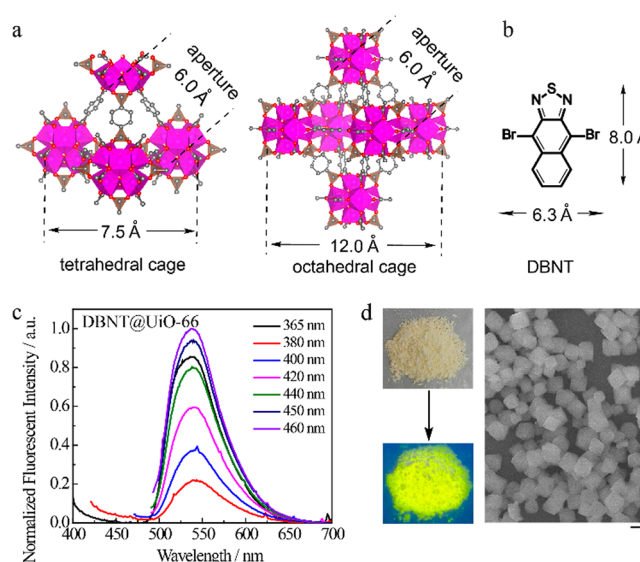


Figure 6. (a) The crystal structure of UiO-66 indicating sizes of aperture and cavity. (b) The molecular structure and dimension of DBNT. (c) PL spectra of the DBNT@UiO-66 nanocomposites in solid state as a function of excitation wavelength. (d) Photographs of DBNT@UiO-66 nanocomposite under daylight (top left) and photoexcitation (bottom left) and SEM image of the DBNT@UiO-66 nanocrystals (scale bar: 200 nm).

continuing research in this very exciting area will undoubtedly promote and facilitate the advancement of LMOFs and their applications in energy-related areas.

1. Chromophoric Ligand-Based LMOFs. Although it remains crucial to synthesize new chromophoric ligands with high quantum efficiency for LMOF preparation, other strategies, such as postsynthetic ligand modification^{53,54} and ligand installation,^{3,55–57} are also very important concurrent approaches for the following reasons: (i) some chromophoric ligands with extremely high photoluminescent performance are very difficult to incorporate directly in LMOFs synthesis, and (ii) postsynthetic modification and ligand installation permit excellent control and flexibility over the synthesis and targeted properties of the resulting LMOFs.

2. Host–Guest-Based LMOFs. Hundreds of thousands of known MOFs can be used as host structures, and nearly limitless luminescent guest species with compatible parameters can be encapsulated/trapped *in situ* into these MOFs. In forming these guest@MOF composites, several important factors must be taken into consideration: the relative dimensions of the guest and MOF pore structure, the stability of the guests, and the overall quantum efficiency of the composites. It is therefore crucial to seek high-performance guest species with suitable size, strong resistance to heat and moisture, and high stability toward irradiation. Carbon dots (CDs) represent one of the promising candidates in this area.^{58,59} Future emphasis should be placed on the synthesis of CDs with high quantum yield, especially in the long-wavelength region.

3. Nanocrystalline LMOFs. The development of nanocrystalline LMOFs is an exciting research direction for both morphology/size controlled synthesis and their eventual applications. Nano-LMOFs possess some important features and advantages that bulk LMOFs are lacking. Successfully reducing the size of LMOF particles to the nanoscale will not only endow the crucial solution processability of these

Nano-LMOFs possess some important features and advantages that bulk LMOFs are lacking. Successfully reducing the size of LMOF particles to nanoscale will not only endow the crucial solution processability of these materials for a broad range of applications, including LED device fabrication, but also greatly lessen the mass-transfer limitations and enhance their performance in sensing, catalysis, and many other important commercial processes.

materials for a broad range of applications, including LED device fabrication, but also greatly lessen the mass-transfer limitations and enhance their performance in sensing, catalysis, and many other important commercial processes.^{60,61} Modulator-mediated growth is currently the most commonly used strategy for nanoMOF synthesis. However, because of the nature of chromophoric ligands and synthesis conditions, very few luminescent nanoMOFs have been synthesized to date. Therefore, more efforts should be directed toward the development of nanosized LMOFs. Additionally, universal synthesis methods need to be further explored, as well as the mechanisms behind the nanoscale MOF synthesis.⁶²

AUTHOR INFORMATION

Corresponding Author

Jing Li – Department of Chemistry and Chemical Biology, Rutgers University, Piscataway, New Jersey 08854, United States; Hoffmann Institute of Advanced Materials (HIAM), Shenzhen Polytechnic, Shenzhen 518055, P.R. China; orcid.org/0000-0001-7792-4322; Email: jingli@rutgers.edu

Authors

Xiao-Yuan Liu – Hoffmann Institute of Advanced Materials (HIAM), Shenzhen Polytechnic, Shenzhen 518055, P.R. China; Department of Chemistry and Chemical Biology, Rutgers University, Piscataway, New Jersey 08854, United States; orcid.org/0000-0003-2400-8085

William P. Lustig – Department of Chemistry and Chemical Biology, Rutgers University, Piscataway, New Jersey 08854, United States; orcid.org/0000-0003-0787-3229

Complete contact information is available at:

<https://pubs.acs.org/10.1021/acsenerylett.0c01148>

Author Contributions

[†]X.-Y.L. and W.P.L. contributed equally to this work.

Notes

The authors declare no competing financial interest.

Biographies

Xiao-Yuan Liu received his Ph.D. degree from East China University of Science and Technology in 2018. He joined Prof. Jing Li's group as a postdoctoral fellow in November 2018 supported by Shenzhen Polytechnic. His research focuses on the synthesis of metal–organic

frameworks and nanomaterials with applications in lighting and catalysis.

William P. Lustig received his Ph.D. degree from Rutgers University in 2019 under Professor Jing Li's guidance. His research is centered on investigating luminescence mechanisms in metal organic frameworks and developing new organic chromophore-based luminescent metal organic frameworks with applications as sensor and phosphor materials.

Jing Li is a Distinguished Professor in the Department of Chemistry and Chemical Biology at Rutgers University. Her research focuses on developing new materials for applications in the field of clean, renewable and sustainable energy. She is currently an Associate Editor of *Crystal Growth & Design*. Group link: <https://chem.rutgers.edu/jinglilab>.

ACKNOWLEDGMENTS

Financial support from the National Science Foundation (Grant No. DMR-1507210) is gratefully acknowledged. X.-Y.L. acknowledges the support from Hoffmann Institute of Advanced Materials (HIAM), Shenzhen Polytechnic.

REFERENCES

- (1) Lustig, W. P.; Mukherjee, S.; Rudd, N. D.; Desai, A. V.; Li, J.; Ghosh, S. K. Metal-organic frameworks: functional luminescent and photonic materials for sensing applications. *Chem. Soc. Rev.* **2017**, *46* (11), 3242–3285.
- (2) Mallick, A.; El-Zohry, A. M.; Shekhah, O.; Yin, J.; Jia, J.; Aggarwal, H.; Emwas, A. H.; Mohammed, O. F.; Eddaoudi, M. Unprecedented Ultralow Detection Limit of Amines using a Thiadiazole-Functionalized Zr(IV)-Based Metal-Organic Framework. *J. Am. Chem. Soc.* **2019**, *141* (18), 7245–7249.
- (3) Li, J.; Yuan, S.; Qin, J.-S.; Pang, J.; Zhang, P.; Zhang, Y.; Huang, Y.; Drake, H. F.; Liu, W. R.; Zhou, H.-C. Stepwise Assembly of Turn-on Fluorescence Sensors in Multicomponent Metal–Organic Frameworks for In Vitro Cyanide Detection. *Angew. Chem., Int. Ed.* **2020**, *59*, 9319–9323.
- (4) Hu, Z.; Lustig, W. P.; Zhang, J.; Zheng, C.; Wang, H.; Teat, S. J.; Gong, Q.; Rudd, N. D.; Li, J. Effective Detection of Mycotoxins by a Highly Luminescent Metal-Organic Framework. *J. Am. Chem. Soc.* **2015**, *137* (51), 16209–16215.
- (5) Yin, H. Q.; Wang, X. Y.; Yin, X. B. Rotation Restricted Emission and Antenna Effect in Single Metal-Organic Frameworks. *J. Am. Chem. Soc.* **2019**, *141* (38), 15166–15173.
- (6) Han, M.-L.; Wen, G.-X.; Dong, W.-W.; Zhou, Z.-H.; Wu, Y.-P.; Zhao, J.; Li, D.-S.; Ma, L.-F.; Bu, X. A heterometallic sodium–europium-cluster-based metal–organic framework as a versatile and water-stable chemosensor for antibiotics and explosives. *J. Mater. Chem. C* **2017**, *5* (33), 8469–8474.
- (7) Zhou, Z. H.; Dong, W. W.; Wu, Y. P.; Zhao, J.; Li, D. S.; Wu, T.; Bu, X. H. Ligand-Controlled Integration of Zn and Tb by Photoactive Terpyridyl-Functionalized Tricarboxylates as Highly Selective and Sensitive Sensors for Nitrofurans. *Inorg. Chem.* **2018**, *57* (7), 3833–3839.
- (8) Sun, C. Y.; Wang, X. L.; Zhang, X.; Qin, C.; Li, P.; Su, Z. M.; Zhu, D. X.; Shan, G. G.; Shao, K. Z.; Wu, H.; Li, J. Efficient and tunable white-light emission of metal-organic frameworks by iridium-complex encapsulation. *Nat. Commun.* **2013**, *4*, 2717.
- (9) Gong, Q.; Hu, Z.; Deibert, B. J.; Emge, T. J.; Teat, S. J.; Banerjee, D.; Mussman, B.; Rudd, N. D.; Li, J. Solution processable MOF yellow phosphor with exceptionally high quantum efficiency. *J. Am. Chem. Soc.* **2014**, *136* (48), 16724–16727.
- (10) Cui, Y.; Song, T.; Yu, J.; Yang, Y.; Wang, Z.; Qian, G. Dye Encapsulated Metal-Organic Framework for Warm-White LED with High Color-Rendering Index. *Adv. Funct. Mater.* **2015**, *25* (30), 4796–4802.

- (11) Lustig, W. P.; Wang, F.; Teat, S. J.; Hu, Z.; Gong, Q.; Li, J. Chromophore-Based Luminescent Metal–Organic Frameworks as Lighting Phosphors. *Inorg. Chem.* **2016**, *55* (15), 7250–7256.
- (12) Chen, Y.; Yu, B.; Cui, Y.; Xu, S.; Gong, J. Core–Shell Structured Cyclodextrin Metal–Organic Frameworks with Hierarchical Dye Encapsulation for Tunable Light Emission. *Chem. Mater.* **2019**, *31* (4), 1289–1295.
- (13) Wang, Z.; Zhu, C.-Y.; Mo, J.-T.; Fu, P.-Y.; Zhao, Y.-W.; Yin, S.-Y.; Jiang, J.-J.; Pan, M.; Su, C.-Y. White-Light Emission from Dual-Way Photon Energy Conversion in a Dye-Encapsulated Metal–Organic Framework. *Angew. Chem., Int. Ed.* **2019**, *58*, 9752–9757.
- (14) Deng, J.; Wang, K.; Wang, M.; Yu, P.; Mao, L. Mitochondria Targeted Nanoscale Zeolitic Imidazole Framework-90 for ATP Imaging in Live Cells. *J. Am. Chem. Soc.* **2017**, *139* (16), 5877–5882.
- (15) Zhang, Z.; Sang, W.; Xie, L.; Dai, Y. Metal-organic frameworks for multimodal bioimaging and synergistic cancer chemotherapy. *Coord. Chem. Rev.* **2019**, *399*, 213022.
- (16) Park, J.; Jiang, Q.; Feng, D.; Mao, L.; Zhou, H. C. Size-Controlled Synthesis of Porphyrinic Metal–Organic Framework and Functionalization for Targeted Photodynamic Therapy. *J. Am. Chem. Soc.* **2016**, *138* (10), 3518–3525.
- (17) Dolgoplova, E. A.; Berseneva, A. A.; Faillace, M. S.; Ejegbavwo, O. A.; Leith, G. A.; Choi, S. W.; Gregory, H. N.; Rice, A. M.; Smith, M. D.; Chruszcz, M.; Garashchuk, S.; Myhre, K.; Shustova, N. B. Confinement-Driven Photophysics in Cages, Covalent–Organic Frameworks, Metal–Organic Frameworks, and DNA. *J. Am. Chem. Soc.* **2020**, *142* (10), 4769–4783.
- (18) Rice, A. M.; Martin, C. R.; Galitskiy, V. A.; Berseneva, A. A.; Leith, G. A.; Shustova, N. B. Photophysics Modulation in Photo-switchable Metal–Organic Frameworks. *Chem. Rev.* **2019**. DOI: 10.1021/acs.chemrev.9b00350
- (19) White, K. A.; Chengelis, D. A.; Gogick, K. A.; Stehman, J.; Rosi, N. L.; Petoud, S. Near-Infrared Luminescent Lanthanide MOF Barcodes. *J. Am. Chem. Soc.* **2009**, *131* (50), 18069–18071.
- (20) Rao, X.; Huang, Q.; Yang, X.; Cui, Y.; Yang, Y.; Wu, C.; Chen, B.; Qian, G. Color tunable and white light emitting Tb³⁺ and Eu³⁺ doped lanthanide metal–organic framework materials. *J. Mater. Chem.* **2012**, *22* (7), 3210–3214.
- (21) Cui, Y.; Chen, B.; Qian, G. Lanthanide metal-organic frameworks for luminescent sensing and light-emitting applications. *Coord. Chem. Rev.* **2014**, *273–274*, 76–86.
- (22) Yin, H. Q.; Yin, X. B. Metal–Organic Frameworks with Multiple Luminescence Emissions: Designs and Applications. *Acc. Chem. Res.* **2020**, *53* (2), 485–495.
- (23) Wu, Y. P.; Xu, G. W.; Dong, W. W.; Zhao, J.; Li, D. S.; Zhang, J.; Bu, X. Anionic Lanthanide MOFs as a Platform for Iron-Selective Sensing, Systematic Color Tuning, and Efficient Nanoparticle Catalysis. *Inorg. Chem.* **2017**, *56* (3), 1402–1411.
- (24) Wei, Z.; Gu, Z. Y.; Arvapally, R. K.; Chen, Y. P.; McDougald, R. N., Jr.; Ivy, J. F.; Yakovenko, A. A.; Feng, D.; Omary, M. A.; Zhou, H. C. Rigidifying fluorescent linkers by metal-organic framework formation for fluorescence blue shift and quantum yield enhancement. *J. Am. Chem. Soc.* **2014**, *136* (23), 8269–8276.
- (25) Hu, Z.; Huang, G.; Lustig, W. P.; Wang, F.; Wang, H.; Teat, S. J.; Banerjee, D.; Zhang, D.; Li, J. Achieving exceptionally high luminescence quantum efficiency by immobilizing an AIE molecular chromophore into a metal-organic framework. *Chem. Commun.* **2015**, *51* (15), 3045–3048.
- (26) Cornelio, J.; Zhou, T. Y.; Alkas, A.; Telfer, S. G. Systematic Tuning of the Luminescence Output of Multicomponent Metal–Organic Frameworks. *J. Am. Chem. Soc.* **2018**, *140* (45), 15470–15476.
- (27) Newsome, W. J.; Ayad, S.; Cordova, J.; Reinheimer, E. W.; Campiglia, A. D.; Harper, J. K.; Hanson, K.; Uribe-Romo, F. J. Solid State Multicolor Emission in Substitutional Solid Solutions of Metal–Organic Frameworks. *J. Am. Chem. Soc.* **2019**, *141* (28), 11298–11303.
- (28) Lan, A.; Li, K.; Wu, H.; Olson, D. H.; Emge, T. J.; Ki, W.; Hong, M.; Li, J. A Luminescent Microporous Metal–Organic Framework for the Fast and Reversible Detection of High Explosives. *Angew. Chem., Int. Ed.* **2009**, *48* (13), 2334–2338.
- (29) Pramanik, S.; Zheng, C.; Zhang, X.; Emge, T. J.; Li, J. New Microporous Metal–Organic Framework Demonstrating Unique Selectivity for Detection of High Explosives and Aromatic Compounds. *J. Am. Chem. Soc.* **2011**, *133* (12), 4153–4155.
- (30) Wen, Y.; Sheng, T.; Zhu, X.; Zhuo, C.; Su, S.; Li, H.; Hu, S.; Zhu, Q. L.; Wu, X. Introduction of Red-Green-Blue Fluorescent Dyes into a Metal–Organic Framework for Tunable White Light Emission. *Adv. Mater.* **2017**, *29*, 1700778.
- (31) Allendorf, M. D.; Bauer, C. A.; Bhakta, R. K.; Houk, R. J. Luminescent metal-organic frameworks. *Chem. Soc. Rev.* **2009**, *38* (5), 1330–1352.
- (32) Cui, Y.; Yue, Y.; Qian, G.; Chen, B. Luminescent functional metal-organic frameworks. *Chem. Rev.* **2012**, *112* (2), 1126–1162.
- (33) Lustig, W. P.; Li, J. Luminescent metal–organic frameworks and coordination polymers as alternative phosphors for energy efficient lighting devices. *Coord. Chem. Rev.* **2018**, *373*, 116–147.
- (34) Hu, Z.; Deibert, B. J.; Li, J. Luminescent metal-organic frameworks for chemical sensing and explosive detection. *Chem. Soc. Rev.* **2014**, *43* (16), 5815–5840.
- (35) Zhang, Y.; Yuan, S.; Day, G.; Wang, X.; Yang, X.; Zhou, H.-C. Luminescent sensors based on metal-organic frameworks. *Coord. Chem. Rev.* **2018**, *354*, 28–45.
- (36) Wu, S.; Min, H.; Shi, W.; Cheng, P. Multicenter Metal–Organic Framework-Based Ratiometric Fluorescent Sensors. *Adv. Mater.* **2020**, *32* (3), 1805871.
- (37) Chen, L.; Liu, D.; Peng, J.; Du, Q.; He, H. Ratiometric fluorescence sensing of metal-organic frameworks: Tactics and perspectives. *Coord. Chem. Rev.* **2020**, *404*, 213113.
- (38) Dolgoplova, E. A.; Rice, A. M.; Martin, C. R.; Shustova, N. B. Photochemistry and photophysics of MOFs: steps towards MOF-based sensing enhancements. *Chem. Soc. Rev.* **2018**, *47* (13), 4710–4728.
- (39) Zhang, Q.; Su, J.; Feng, D.; Wei, Z.; Zou, X.; Zhou, H. C. Piezofluorochromic Metal–Organic Framework: A Microscissor Lift. *J. Am. Chem. Soc.* **2015**, *137* (32), 10064–10067.
- (40) Lustig, W. P.; Teat, S. J.; Li, J. Improving LMOF luminescence quantum yield through guest-mediated rigidification. *J. Mater. Chem. C* **2019**, *7* (46), 14739–14744.
- (41) Lustig, W. P.; Shen, Z.; Teat, S. J.; Javed, N.; Velasco, E.; O’Carroll, D. M.; Li, J. Rational design of a high-efficiency, multivariate metal–organic framework phosphor for white LED bulbs. *Chem. Sci.* **2020**, *11* (7), 1814–1824.
- (42) Tang, Y.; Xia, T.; Song, T.; Cui, Y.; Yang, Y.; Qian, G. Efficient Energy Transfer within Dyes Encapsulated Metal–Organic Frameworks to Achieve High Performance White Light-Emitting Diodes. *Adv. Opt. Mater.* **2018**, *6* (24), 1800968.
- (43) He, L.; Wang, T.; An, J.; Li, X.; Zhang, L.; Li, L.; Li, G.; Wu, X.; Su, Z.; Wang, C. Carbon nanodots@zeolitic imidazolate framework-8 nanoparticles for simultaneous pH-responsive drug delivery and fluorescence imaging. *CrystEngComm* **2014**, *16* (16), 3259–3263.
- (44) Xie, W.; He, W. W.; Du, D. Y.; Li, S. L.; Qin, J. S.; Su, Z. M.; Sun, C. Y.; Lan, Y. Q. A stable Alq3@MOF composite for white-light emission. *Chem. Commun.* **2016**, *52* (16), 3288–3291.
- (45) Wang, Z.; Wang, Z.; Lin, B.; Hu, X.; Wei, Y.; Zhang, C.; An, B.; Wang, C.; Lin, W. Warm-White-Light-Emitting Diode Based on a Dye-Loaded Metal–Organic Framework for Fast White-Light Communication. *ACS Appl. Mater. Interfaces* **2017**, *9* (40), 35253–35259.
- (46) Chen, W.; Zhuang, Y.; Wang, L.; Lv, Y.; Liu, J.; Zhou, T. L.; Xie, R. J. Color-Tunable and High-Efficiency Dye-Encapsulated Metal–Organic Framework Composites Used for Smart White-Light-Emitting Diodes. *ACS Appl. Mater. Interfaces* **2018**, *10* (22), 18910–18917.
- (47) Xie, W.; Qin, J.-S.; He, W.-W.; Shao, K.-Z.; Su, Z.-M.; Du, D.-Y.; Li, S.-L.; Lan, Y.-Q. Encapsulation of an iridium complex in a metal–organic framework to give a composite with efficient white light emission. *Inorg. Chem. Front.* **2017**, *4* (3), 547–552.

(48) Glembocky, V.; Frenette, M.; Mottillo, C.; Durantini, A. M.; Gostick, J.; Strukil, V.; Friscic, T.; Cosa, G. Highly Photostable and Fluorescent Microporous Solids Prepared via Solid-State Entrapment of Boron Dipyrromethene Dyes in a Nascent Metal-Organic Framework. *J. Am. Chem. Soc.* **2018**, *140*, 16882–16887.

(49) Liu, X. Y.; Xing, K.; Li, Y.; Tsung, C. K.; Li, J. Three Models To Encapsulate Multicomponent Dyes into Nanocrystal Pores: A New Strategy for Generating High-Quality White Light. *J. Am. Chem. Soc.* **2019**, *141* (37), 14807–14813.

(50) Liu, X. Y.; Li, Y.; Tsung, C. K.; Li, J. Encapsulation of yellow phosphors into nanocrystalline metal-organic frameworks for blue-excitable white light emission. *Chem. Commun.* **2019**, *55* (72), 10669–10672.

(51) Liu, X. Y.; Lo, W. S.; Wu, C.; Williams, B. P.; Luo, L.; Li, Y.; Chou, L. Y.; Lee, Y.; Tsung, C. K. Tuning Metal-Organic Framework Nanocrystal Shape through Facet-Dependent Coordination. *Nano Lett.* **2020**, *20* (3), 1774–1780.

(52) Liu, X. Y.; Zhang, F.; Goh, T. W.; Li, Y.; Shao, Y. C.; Luo, L.; Huang, W.; Long, Y. T.; Chou, L. Y.; Tsung, C. K. Using a Multi-Shelled Hollow Metal-Organic Framework as a Host to Switch the Guest-to-Host and Guest-to-Guest Interactions. *Angew. Chem., Int. Ed.* **2018**, *57* (8), 2110–2114.

(53) Wang, Z.; Cohen, S. M. Postsynthetic modification of metal-organic frameworks. *Chem. Soc. Rev.* **2009**, *38* (5), 1315–1329.

(54) Tanabe, K. K.; Cohen, S. M. Postsynthetic modification of metal-organic frameworks—a progress report. *Chem. Soc. Rev.* **2011**, *40* (2), 498–519.

(55) Yuan, S.; Lu, W.; Chen, Y. P.; Zhang, Q.; Liu, T. F.; Feng, D.; Wang, X.; Qin, J.; Zhou, H. C. Sequential linker installation: precise placement of functional groups in multivariate metal-organic frameworks. *J. Am. Chem. Soc.* **2015**, *137* (9), 3177–3180.

(56) Zhang, X.; Frey, B. L.; Chen, Y. S.; Zhang, J. Topology-Guided Stepwise Insertion of Three Secondary Linkers in Zirconium Metal-Organic Frameworks. *J. Am. Chem. Soc.* **2018**, *140* (24), 7710–7715.

(57) Pang, J.; Yuan, S.; Qin, J. S.; Lollar, C. T.; Huang, N.; Li, J.; Wang, Q.; Wu, M.; Yuan, D.; Hong, M.; Zhou, H. C. Tuning the Ionicity of Stable Metal-Organic Frameworks through Ionic Linker Installation. *J. Am. Chem. Soc.* **2019**, *141* (7), 3129–3136.

(58) Yuan, F.; Wang, Z.; Li, X.; Li, Y.; Tan, Z.; Fan, L.; Yang, S. Bright Multicolor Bandgap Fluorescent Carbon Quantum Dots for Electroluminescent Light-Emitting Diodes. *Adv. Mater.* **2017**, *29*, 1604436.

(59) Lim, S. Y.; Shen, W.; Gao, Z. Carbon quantum dots and their applications. *Chem. Soc. Rev.* **2015**, *44* (1), 362–381.

(60) Wang, S.; McGuirk, C. M.; d'Aquino, A.; Mason, J. A.; Mirkin, C. A. Metal-Organic Framework Nanoparticles. *Adv. Mater.* **2018**, *30* (37), 1800202.

(61) Marshall, C. R.; Staudhammer, S. A.; Brozek, C. K. Size control over metal-organic framework porous nanocrystals. *Chem. Sci.* **2019**, *10* (41), 9396–9408.

(62) Wang, X. G.; Cheng, Q.; Yu, Y.; Zhang, X. Z. Controlled Nucleation and Controlled Growth for Size Predictable Synthesis of Nanoscale Metal-Organic Frameworks (MOFs): A General and Scalable Approach. *Angew. Chem., Int. Ed.* **2018**, *57* (26), 7836–7840.